Inorg. Chem. **2004**, *43*, 5714–5724

Pyridine Substituted N-Heterocyclic Carbene Ligands as Supports for Au(I)–Ag(I) Interactions: Formation of a Chiral Coordination Polymer

Vincent J. Catalano,* Mark A. Malwitz, and Anthony O. Etogo

Department of Chemistry, University of Nevada, Reno, Nevada 89557

Received March 24, 2004

Reaction of 1,3-bis(2-pyridinylmethyl)-1H-imidazolium tetrafluoroborate, $[H(pyCH_2)_2im]BF_4$, with silver oxide in dichloromethane readily yields $[Ag((pyCH_2)_2im)_2]BF_4$, **1·BF$_4$**. **1·BF$_4$** is converted to the analogous Au(I)-containing species, $[Au((pyCH_2)_2im)_2]BF_4$, **3**, by a simple carbene transfer reaction in dichloromethane. Further treatment with two equivalents of $AgBF_4$ produces the trimetallic species $[AuAg_2((pyCH_2)_2im)_2(NCCH_3)_2](BF_4)_3$, **4**, which contains two silver ions each coordinated to the pyridine moieties on one carbene ligand and to an acetonitrile molecule in a T-shaped fashion. Monometallic $[Ag((py)_2im)_2]BF_4$, **5**, and $[Au((py)_2im)_2]BF_4$, **6**, are made analogously to **1·BF$_4$** and **3** starting from 1,3-bis(2-pyridyl)-imidazol-2-ylidene tetrafluoroborate, $[H(py)_2im]BF_4$. Addition of excess $AgBF_4$ to **6** yields the helical mixed-metal polymer, $\{[AuAg((py)_2im)_2(NCCH_3)](BF_4)_2\}_n$, **7** which contains an extended Au(I)–Ag(I) chain with short metal–metal separations of 2.8359(4) and 2.9042(4) Å. Colorless, monometallic $[Hg((pyCH_2)_2im)_2](BF_4)_2$, **8**, is easily produced by refluxing $[H(pyCH_2)_2im)]BF_4$ with $Hg(OAc)_2$ in acetonitrile. The related quinolyl-substituted imidazole, $[H(quinCH_2)_2im]PF_6$, is produced analogously to $[H(pyCH_2)_2im]BF_4$. $[Hg((quinCH_2)_2im)_2](PF_6)_2$, **9**, is isolated in good yield as a white solid from the reaction of $Hg(OAc)_2$ and $[H(quinCH_2)_2im]PF_6$. The reaction of $[H(quinCH_2)_2im]PF_6$ with excess Ag_2O produces the triangulo-cluster $[Ag_3((quinCH_2)_2im)_3](PF_6)_3$, **11**. All of these complexes were studied by ^1H NMR spectroscopy, and complexes **3**–**9** were additionally characterized by X-ray crystallography. These complexes are photoluminescent in the solid state and in solution with spectra that closely resemble those of the ligand precursor.

Introduction

Nonbonding interactions between closed-shell metals,[1] particularly d^{10}-d,[10] often produce materials with interesting luminescent properties.[2] Among the most studied are the aurophilic Au(I)−Au(I)[3] interactions resulting from aggregation of linear, two-coordinate gold monomers in the solid state or those induced by the incorporation of bridging ligands.[4] In the former, aggregation in the solid state produces several structural motifs including the periodic distribution of discrete dimers,[5] extended zigzag arrays[6] of Au(I) centers with short metal−metal separations, and three-dimensional networks[7] of metal centers. A common feature to all of these solid-state systems is that the Au−Au interactions are usually lost upon dissolution. To counter this, a huge variety of bidentate or multidentate ligands, usually phosphines,[8] are

* Author to whom correspondence should be addressed. E-mail: vjc@unr.edu.

(1) (a) Fernández, E. J.; López-de-Luzuriaga, J. M.; Monge, M.; Olmos, M. E.; Pérez, J.; Laguna, A.; Mohamed, A. A.; Fackler, J. P., Jr. *J. Am. Chem. Soc.* **2003**, 125, 2022. (b) Fernández, E. J.; Laguna, A.; López-de-Luzuriaga, J. M.; Mendizabal, F.; Monge, M.; Olmos, M. E., Pérez, J. *Chem. Eur. J.* **2003**, *9*, 456. (c) Fernández, E. J.; Laguna, A.; López-de-Luzuriaga, J. M.; Olmos, M. E.; Pérez, J. *Chem. Commun.* **2003**, 1760.

(2) (a) White-Morris, R. L.; Olmstead, M. M.; Jiang, F.; Tinti, D. S.; Balch, A. L. *J. Am. Chem. Soc.* **2002**, *124*, 2327. (b) Vickery, J. C.; Olmstead, M. M.; Fung, E. Y.; Balch, A. L. *Angew. Chem., Int. Ed. Engl.* **1997**, *36*, 1179. (c) Mansour, M. A.; Connick, W. B.; Lachicotte, R. J.; Gysling, H. J.; Eisenberg, R. J. *J. Am. Chem. Soc.* **1998**, *120*, 1329.

(3) (a) *Gold: Progress in Chemistry, Biochemistry and Technology*; Schmidbaur, H., Ed.; Wiley: New York, 1999. (b) Schmidbaur, H. *Nature* **2001**, *413*, 31. (c) Schmidbaur, H. *Gold Bull.* **1990**, *23*, 11.

(4) (a) Lee, Y.-A.; Eisenberg, R. *J. Am. Chem. Soc.* **2003**, *125*, 7778. (b) Leung, K. H.; Phillips, D. L.; Mao, Z.; Che, C.-M.; Miskowski, V. M.; Chan, C.-K. *Inorg. Chem.* **2002**, *41*, 2054

(5) (a) White-Morris, R. L.; Olmstead, M. M.; Balch, A. L.; Elbjeirami, O.; Omary, M. A. *Inorg. Chem.* **2003**, *42*, 6741. (b) Hamel, A.; Mitzel, N. W.; Schmidbaur, H. *J. Am. Chem. Soc.* **2001**, *123*, 5106.

(6) White-Morris, R. L.; Olmstead, M. M.; Balch, A. L. *J. Am. Chem. Soc.* **2003**, *125*, 1033.

(7) (a) Hunks, W. J.; Jennings, M. C.; Puddephatt, R. J. *Inorg. Chem.* **2002**, *41*, 4590. (b) Puddephatt, R. J. *Coord. Chem. Rev.* **2001**, *216−217*, 313. (c) Leznoff, D. B.; Xue, B.-Y.; Batchelor, R. J.; Einstein, F. W. B.; Patrick, B. O. *Inorg. Chem.* **2001**, *40*, 6026.

(8) Cotton, F. A.; Hong, B. *Prog. Inorg. Chem.* **1992**, *40*, 179.

10.1021/ic049604k CCC: $27.50
Published on Web 08/04/2004

Scheme 1

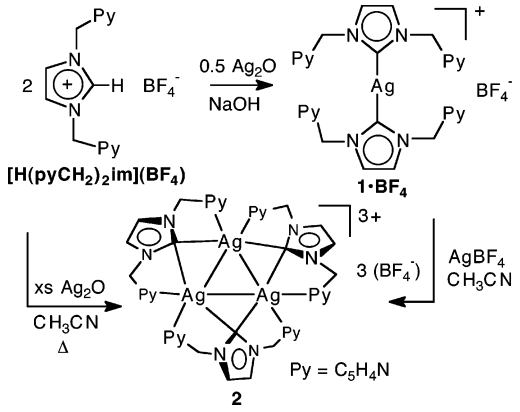

employed to maintain the metal−metal interaction in solution, and the resulting complexes remain photoluminescent in solution.

Investigations into mixed-metal interactions[9,10] are also becoming more popular, and many examples of complexes containing short argento-aurophilic[11,22] contacts have been reported recently. In many of these systems the resulting mixed-metal separation is shorter than the corresponding distance in the homometallic analogues. The shortened separation and increased stability is attributed to the introduction of a dipolar interaction between the dissimilar metals augmenting the dispersion forces[12] believed to be the primary attractive force maintaining these assemblies.

Like phosphines, N-heterocyclic carbene (NHC) ligands are excellent ligands for late transition metals and have metal−ligand bond strengths and sigma donor properties rivaling most phosphines.[13] Their ease of preparation and functionalization[14] makes these ligands ideally suited for stabilizing multimetallic architectures. Notably, Herrmann and co-workers[15] have extensively developed the transition metal chemistry of NHC ligands particularly in the area of developing C−C coupling catalysts.

Earlier we reported the application of the 2-picolyl substituted NHC ligand toward maintaining Ag(I)−Ag(I) interactions.[16] The simple reaction (Scheme 1) of the NHC precursor, 1,3-bis(2-pyridinylmethyl)-1H-imidazolium tetrafluoroborate, $[H(pyCH_2)_2im]BF_4$ with silver oxide in acetonitrile produces the unusual triangulo-Ag_3 cluster, $[Ag_3((pyCH_2)_2im)_3](BF_4)_3$, **2**, containing unusually short (2.72 to 2.78 Å) Ag−Ag separations spanned by bridging carbene ligands. This robust species is intensely photoluminescent. We have now extended this chemistry to mixed

Scheme 2

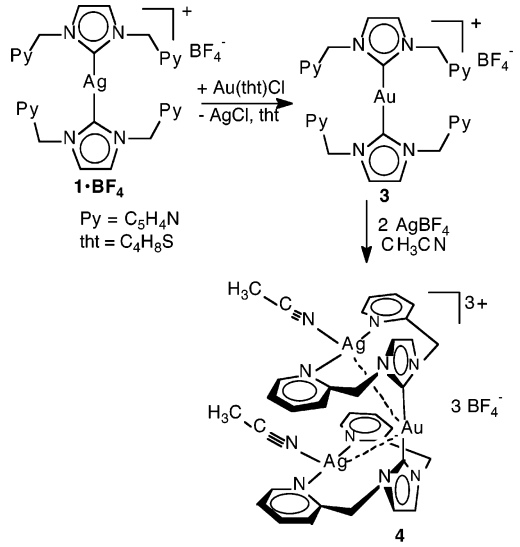

Scheme 3

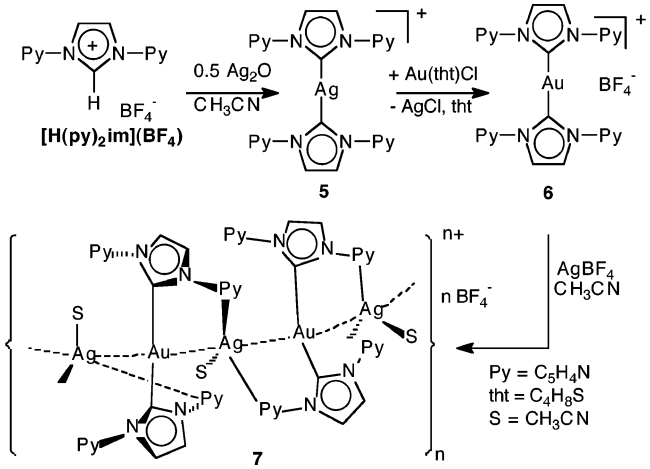

metal systems and explored similar chemistry with the closely related pyridyl-substituted NHCs.

Results

Deprotonation of the known imidazolium salt, $[H(pyCH_2)_2im]BF_4$,[17] with Ag_2O in CH_2Cl_2 readily produces the colorless, homoleptic $[Ag((pyCH_2)_2im)_2]BF_4$ complex, **1·BF$_4$**, in high yield and high purity. According to Scheme 2, complex **1·BF$_4$** is converted to the analogous Au(I)-containing species, $[Au((pyCH_2)_2im)_2]BF_4$, **3**, by a simple carbene transfer reaction in CH_2Cl_2. Further treatment with two equivalents of $AgBF_4$ produces the trimetallic species $[AuAg_2((pyCH_2)_2im)_2(NCCH_3)_2](BF_4)_3$, **4**, which contains two silver ions each coordinated to the pyridine moieties on one carbene ligand and to an acetonitrile molecule in a T-shaped fashion (vide infra). There is no evidence of polymer formation in this reaction.

As shown in Scheme 3, the absence of the methylene spacer in the carbene ligand reduces the flexibility of the

(9) Bardají, M.; Laguna, A. *Eur. J. Inorg. Chem.* **2003**, 3069.
(10) Catalano, V. J.; Bennett, B. L.; Malwitz, M. A, Yson, R. L.; Kar, H. M.; Muratidis, S.; Horner, S. J. *Comment. Inorg. Chem.* **2003**, *24*, 39.
(11) Catalano, V. J.; Horner, S. J. *Inorg. Chem.* **2003**, *42*, 8430.
(12) Mendizabal, F.; Pyykkö, P.; Runeberg, *Chem. Phys. Lett.* **2003**, *370*, 733. (b) Runeberg, N.; Schütz, M.; Werner, H.-J. *J. Chem. Phys.* **1999**, *110*, 7210.
(13) Lee, M.-T.; Hu, C.-H. *Organometallics* **2004**, *23*, 976.
(14) Bourissou, D.; Guerret, O.; Gabbaï, F. P.; Bertrand, G. *Chem. Rev.* **2000**, *100*, 39.
(15) (a) Herrmann, W. A.; Weskamp, T.; Böhm, V. P. W. *Adv. Organomet. Chem.* **2001**, *48*, 1. (b) Weskamp, T.; Böhm, V. P. W.; Herrmann, W. A. *J. Organomet. Chem.* **2000**, *600*, 12. (c) Herrmann, W. A.; Köcher, C. *Angew. Chem., Int. Ed. Engl.* **1997**, *36*, 2162.
(16) Catalano, V. J.; Malwitz, M. A. *Inorg. Chem.* **2003**, *42*, 5483.
(17) Magill, A. M.; McGuinness, D. S.; Cavell, K. J.; Britovsek, G. J. P.; Gibson, V. C.; White, A. J. P.; Williams, D. J.; White, A. H.; Skelton, B. W. *J. Organomet. Chem.* **2001**, *617−618*, 546.

Scheme 4

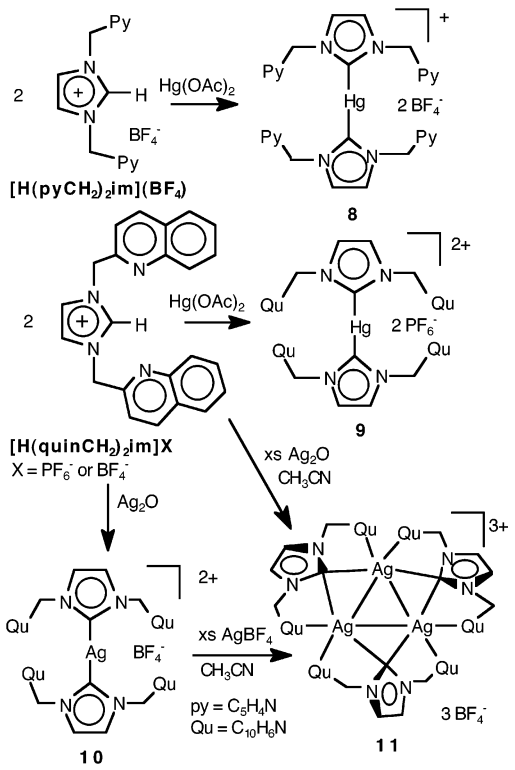

pyridine group which in turn, influences the multimetallic coordination chemistry. Starting from 1,3-bis(2-pyridyl)-imidazol-2-ylidene tetrafluoroborate, $[H(py)_2im]BF_4$, the monometallic $[Ag((py)_2im)_2]BF_4$, **5**, and $[Au((py)_2im)_2]BF_4$, **6**, are made analogously to **1·BF4** and **3**, respectively. Addition of excess $AgBF_4$ to **6** does not yield the anticipated trimetallic species. Rather, the helical mixed-metal polymer, $\{[AuAg((py)_2im)_2(NCCH_3)](BF_4)_2\}_n$, **7**, is isolated. The formation of **7** is independent of reaction conditions and stoichiometry. The same product is obtained whether one to four equivalents of $AgBF_4$ are added to **6** at room temperature or while refluxing in acetonitrile.

The Hg(II) chemistry of $[H(pyCH_2)_2im)]BF_4$ is simple. Colorless $[Hg((pyCH_2)_2im)_2](BF_4)_2$, **8**, is easily produced by refluxing $[H(pyCH_2)_2im)]BF_4$ with $Hg(OAc)_2$ in acetonitrile. Addition of $AgBF_4$ to this material does not produce the anticipated trimetallic species, and only the respective starting materials are recovered. Likewise, the closely related quinolyl-substituted imidazole, $[H(quinCH_2)_2im]PF_6$ or $[H(quinCH_2)_2$-im**]**BF_4, produced analogously to $[H(pyCH_2)_2im]BF_4$, exhibits reactivity similar to the pyridine analogue. The monometallic $[Hg((quinCH_2)_2im)_2](PF_6)_2$, **9**, is isolated in good yield as a white solid from the reaction of mercuric acetate and $[H(quinCH_2)_2im]PF_6$. The Ag(I) chemistry directly mirrors the chemistry reported in Scheme 1 with the reaction of $[H(quinCH_2)_2im]BF_4$ with excess Ag_2O producing the triangulo-cluster $[Ag_3((quinCH_2)_2im)_3](BF_4)_3$, **11**, which can also be made by treating the monometallic species, $[Ag((quinCH_2)_2im)_2](BF_4)$, **10**, with two equivalents of $AgBF_4$.

The aforementioned complexes were studied by ^{1}H NMR spectroscopy, and their spectra are consistent with their proposed formulation. In CD_3CN $[Au((pyCH_2)_2im)_2]BF_4$, **3**, shows six proton resonances with the diagnostic methylene and imidazolium backbone resonances appearing as singlets at 5.41 and 7.30 ppm, respectively. Upon coordination of two Ag(I) ions to form $[AuAg_2((pyCH_2)_2im)_2(NCCH_3)_2](BF_4)_3$, **4**, these resonances shift downfield to 5.62 and 7.55 ppm, respectively, along with a similar shift for the pyridine resonances (see Experimental Section). The coordinated acetonitrile molecules, evident from the X-ray crystallography (vide infra), are not observed and are likely exchanging with the solvent. The ^{1}H NMR spectrum of the mercury complex, $[Hg((pyCH_2)_2im)_2](BF_4)_2$, **8**, is very similar to those of **1** and **3**. The methylene resonance in **8** is observed at 5.49 ppm, and the imidazolium-backbone proton resonance appears at 7.67 ppm. Additionally, this resonance is flanked by ^{199}Hg satellites with a $^4J_{H-Hg}$ of 28 Hz. Similar proton couplings to ^{107}Ag or ^{109}Ag were noticeably absent for all of the silver containing species.

For the $[H(py)_2im]BF_4$ system the changes in coordination produce much more subtle changes in chemical shift. The carbene precursor, $[H(py)_2im]BF_4$, displays four resonances in the aromatic region assigned to the pyridine ring and two singlets in a 2:1 ratio associated with the imidazolium protons at 10.08 and 8.33 ppm. The downfield resonance disappears upon treatment with Ag_2O to produce $[Ag((py)_2im)_2]BF_4$, **5**, and the remaining imidazolium resonance shifts to 8.19 ppm. Conversion to the Au(I) species, **6**, shifts this resonance upfield to 7.92 ppm with only minor changes in the pyridine resonances.

At room temperature the solution state spectrum (CD_3-CN) of **7** is nearly identical to that of **6** with only one pyridine environment observed indicating that this mixed-metal coordination polymer readily dissociates silver ion in solution at room temperature. This process may be facilitated by the presence of a good donor like acetonitrile acting both as a solvent and as a coordinated ligand making the three coordinate Ag(I) center labile. A variable temperature NMR experiment was conducted in acetone because the relatively high freezing point of acetonitrile limited its use as a solvent. At −30 °C the material begins to precipitate from solution without any changes in the NMR spectrum. At −50 °C the resonances begin to broaden, but the inhomogeneity of the sample and low signal-to-noise limit any useful interpretation of the spectrum.

The ^{1}H NMR spectra (CD_3CN) of the quinolyl-substituted imidazole species are very similar to their pyridine analogues. The carbene precursor, $[H(quinCH_2)_2im]PF_6$, shows nine independent resonances with the methylene resonance appearing at 5.71 ppm and the two imidazolium resonances at 7.60 and 8.97 ppm in a 2:1 ratio, respectively. Addition of $Hg(OAc)_2$ to form **9** eliminates the downfield resonance and shifts the methylene resonance to 5.75 ppm and the remaining imidazolium-backbone proton resonance to 7.98 ppm. Like **8** ^{199}Hg satellites are observed in **9** with a similar coupling of 28 Hz. The analogous resonances in compound **10** are shifted slightly upfield at 5.43 and 7.32 ppm, respectively. For the trinuclear species, **11**, the methylene resonance appears as an AB quartet centered at 4.76 ppm, while the

Table 1. Crystallographic Data for Complexes **3**−**7**

	3	**4·2CH$_3$CN**	**5**	**6·2H$_2$O**	**7·CH$_3$CN**
formula	$C_{30}H_{28}AuBF_4N_8$	$C_{38}H_{40}Ag_2AuB_3F_{12}N_{12}$	$C_{26}H_{20}AgBF_4N_8$	$C_{26}H_{24}AuBF_4N_8O_2$	$C_{30}H_{26}AgAuB_2F_8N_{10}$
fw	784.38	1337.94	639.18	764.31	1005.06
crystal system	monoclinic	monoclinic	monoclinic	monoclinic	hexagonal
space group	*C*2/*c*	P2(1)/n	*C*2/*c*	P2(1)/c	P6(5)
a, Å	11.9634(7)	16.253(2)	33.390(4)	14.6707(7)	13.1850(3)
b, Å	12.3560(10)	15.313(2)	7.7862(9)	13.6380(7)	13.1850(3)
c, Å	20.980(2)	19.189(2)	22.606(3)	14.9697(7)	32.5591(12)
α, deg	90	90	90	90	90
β, deg	102.95(2)	92.142(9)	112.408(10)	118.811(1)	90
γ, deg	90	90	90	90	120
V, Å^3	3023.8(4)	4772.4(10)	5433.4(12)	2624.4(2)	4901.9(2)
Z	4	4	8	4	6
temp, K	298(2)	298(2)	100(2)	100(2)	100(2)
R_1, wR_2 (I>2σ(I))	0.0363, 0.0676	0.0685, 0.1173	0.0596, 0.1814	0.0275, 0.0696	0.0248, 0.0503

Table 2. Crystallographic Data for Complexes **8** and **9**

	8·2C$_6$H$_6$	**9·C$_6$H$_6$·CH$_3$CN**
formula	$C_{42}H_{40}B_2F_8HgN_8$	$C_{54}H_{45}F_{12}HgN_9P_2$
fw	1031.03	1310.52
crystal system	triclinic	monoclinic
space group	P-1	P2(1)/n
a, Å	11.224(7)	13.489(3)
b, Å	11.666(2)	28.657(6)
c, Å	18.096(4)	15.063(2)
α, deg	88.07(2)	90
β, deg	82.92(3)	116.552(8)
γ, deg	68.24(4)	90
V, Å^3	2183.8(14)	5208.4(17)
Z	2	4
temp, K	298(2)	90(2)
R_1, wR_2 (I>2σ(I))	0.0439, 0.0942	0.0270, 0.0568

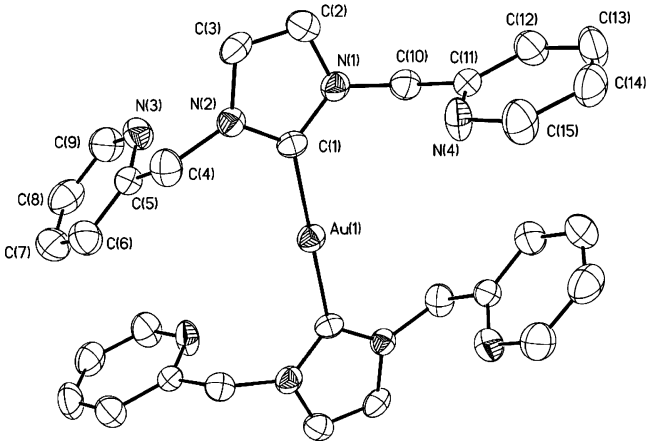

Figure 1. X-ray structural drawing (40%) of the cationic portion of **3** with hydrogen atoms removed for clarity. Only the crystallographically unique portion is labeled.

remaining imidazolium peak moves to 7.48 ppm overlapping an aromatic resonance from the quinolyl group.

Compounds **3**−**9** were additionally characterized by single-crystal X-ray diffraction. Crystallographic data are presented in Tables 1 and 2. As shown in Figure 1 compound **3** crystallizes in the monoclinic space group, *C*2/*c*, with only one-half of the cation and tetrafluoroborate anion residing in the asymmetric unit. The remainder is related by a crystallographic inversion center making the C(1)−Au(1)−C(1A) angle rigorously linear (180°) and the two imidazole rings coplanar. The Au(1)−C(1) distance of 2.021(7) Å is typical for NHC ligands where metal−ligand back-bonding is not observed.[16,18] No short, aurophilic interactions are

Table 3. Selected Bond Distances (Å) and Angles (deg) for **3**

Au(1)−C(1)	2.021(7)	Au(1)−C(1)−N(1)	126.7(5)
C(1)−N(1)	1.344(9)	Au(1)−C(1)−N(2)	127.9(5)
C(1)−N(2)	1.340(8)	C(1)−N(1)−C(2)	110.5(6)
N(1)−C(2)	1.388(9)	C(1)−N(2)−C(3)	111.0(6)
N(2)−C(3)	1.381(9)	N(1)−C(2)−C(3)	106.6(7)
C(2)−C(3)	1.342(10)	N(2)−C(3)−C(2)	106.6(7)

Table 4. Selected Bond Distances (Å) and Angles (deg) for **4**

Au(1)−Ag(1)	3.2197(17)	C(1)−Au(1)−C(16)	175.2(7)
Au(1)−Ag(2)	3.2819(17)	Ag(1)−Au(1)−Ag(2)	63.69(4)
Ag(1)−Ag(2)	3.431(2)	N(3)−Ag(1)−N(4)	167.7(5)
Au(1)−Au(1A)	3.3262(13)	N(3)−Ag(1)−N(9)	89.6(5)
Au(1)−C(1)	1.988(16)	N(4)−Ag(1)−N(9)	91.5(5)
Au(1)−C(16)	1.998(16)	N(7)−Ag(2)−N(8)	161.9(5)
Ag(1)−N(3)	2.253(14)	N(7)−Ag(2)−N(10)	98.7(5)
Ag(1)−N(4)	2.238(13)	N(8)−Ag(2)−N(10)	96.6(5)
Ag(1)−N(9)	2.592(18)	Ag(1)−Au(1)−Au(1A)	148.93(4)
Ag(2)−N(7)	2.234(13)	Ag(2)−Au(1)−Au(1A)	144.40(5)
Ag(2)−N(8)	2.266(14)	Au(1)−Ag(1)−N(9)	172.2(4)
Ag(2)−N(10)	2.590(18)	Au(1)−Ag(2)−N(10)	110.3(4)
Au(1)−Au(1A)	3.3262(13)		

observed, and the shortest intermolecular Au···Au separation is very long at 8.599 Å. The remaining metrical parameters are unremarkable and listed in Table 3.

The incorporation of two Ag(I) atoms into [Au((pyCH_2)$_2$-im)$_2$]BF_4 to form [AuAg_2((pyCH_2)$_2$im)$_2$-(NCCH_3)$_2$]$(BF_4)_3$, **4**, profoundly changes the solid-state structure. Selected bond distances and angles are presented in Table 4. As shown in Figure 2 the pyridine rings of each carbene ligand are splayed back such that they are nearly orthogonal to the imidazole ring and coordinated to a Ag(I) ion in a trans fashion. Each Ag(I) is further coordinated to an acetonitrile molecule giving the metal center an overall T-shaped geometry with N(3)−Ag(1)−N(9), N(4)−Ag(1)−N(9), and N(3)−Ag(1)−N(4) angles of 89.6(5), 91.5(5), and 167.7(5)°, respectively, and N(7)−Ag(2)−N(10), N(8)−Ag(2)−N(10), and N(7)−Ag-(2)−N(8) angles of 98.7(5), 96.6(5), and 161.9(5)°. The coordinated acetonitrile molecules are held weakly to the Ag atoms with long Ag(1)−N(9) and Ag(2)−N(10) distances of 2.592(18) and 2.590(18) Å each. The Ag centers also weakly interact with the Au(I) center with Ag(1)−Au(1) and Ag(2)−Au(1) separations of 3.220(2) and 3.282(2) Å and with each other with a Ag(1)−Ag(2) distance of 3.431(1) Å. The Au(1) remains linearly coordinated to two NHC

(18) Green, J. C.; Scurr, R. G.; Arnold, P. L.; Cloke, F. G. N. *Chem. Commun.* **1997**, 1963.

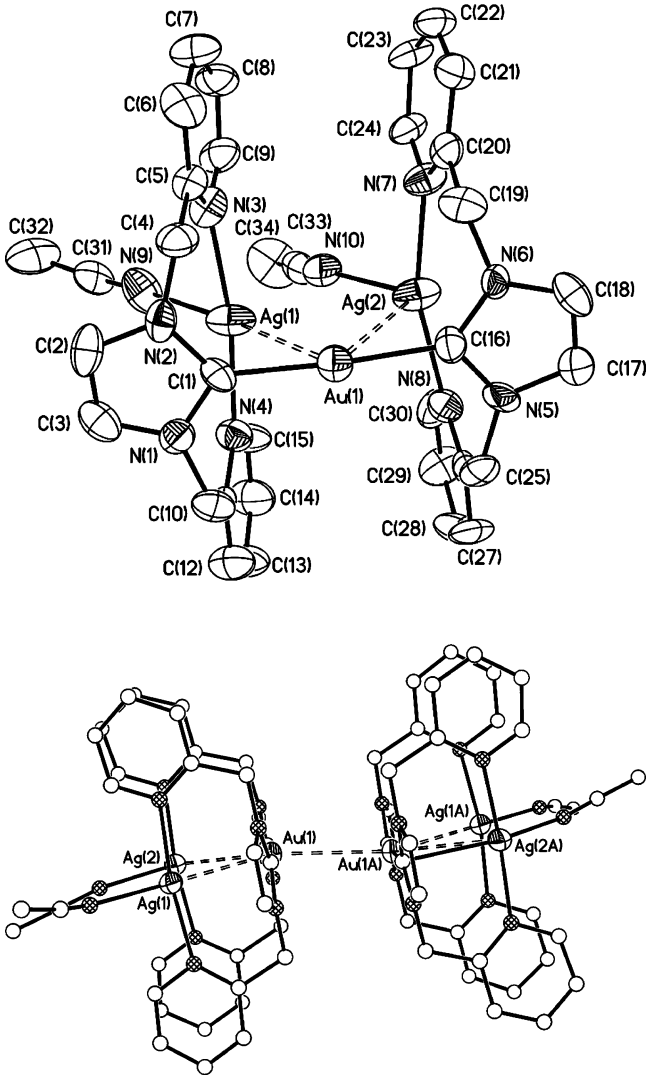

Figure 2. Crystal drawing of cationic portion (top) of **4** with hydrogen atoms removed for clarity. These complexes are held together through a weak intermolecular aurophilic attraction of 3.326(1) Å (bottom). The carbon atoms are represented by open circles, and the nitrogen atoms are depicted with a crosshatch pattern.

ligands with Au(1)−C(1) and Au(1)−C(16) separations of 1.988(16) and 1.998(16) Å, respectively, and a C(1)−Au(1)−C(16) angle of 175.2(7)°. Further, the exposed face of this Au center associates with another cationic complex through a weak aurophilic interaction with a Au···Au separation of 3.326(1) Å.

As expected the crystal structures of $[Ag((py)_2im)_2]BF_4$, **5**, and $[Au((py)_2im)_2]BF_4$, **6**, are very similar. As shown in Figures 3 and 4 and tabulated in Tables 5 and 6, each metal is nearly linearly coordinated to two carbene ligands with C(1)−Ag(1)−C(14) and C(1)−Au(1)−C(14) angles of 176.8(2) and 173.8(1)°, respectively. In **5** the Ag(1)−C(1) and Ag(1)−C(14) separations measure 2.117(5) and 2.106(6) Å, respectively, while in **6** the corresponding Au(1)−C(1) and Au(1)−C(14) separations are slightly shorter at 2.014(4) and 2.022(4) Å, respectively, exemplifying the smaller size of Au versus Ag. The notion that the third row metal is smaller than its second row counterpart was first put forth by Schmidbaur and is attributed to relativistic effects contracting

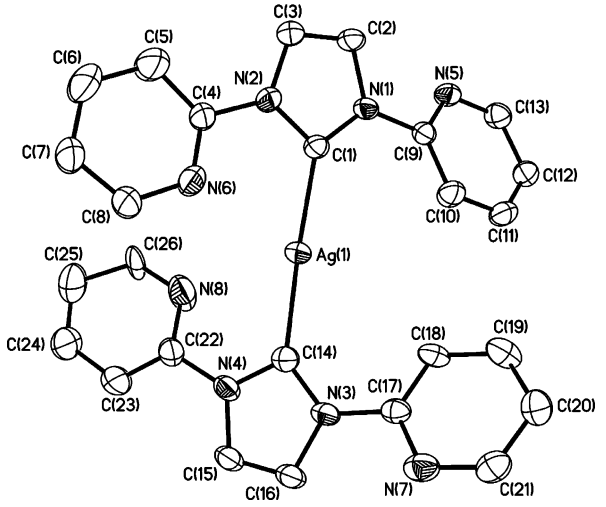

Figure 3. Thermal ellipsoid plot (50%) of cationic portion of **5** with hydrogen atoms removed for clarity.

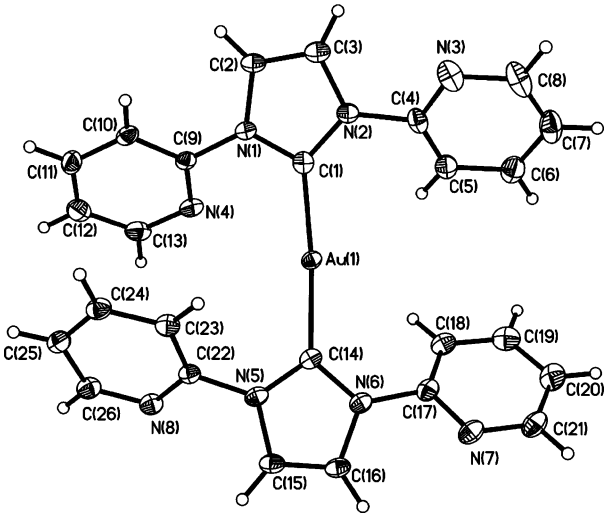

Figure 4. Thermal ellipsoid plot (50%) of cationic portion of **6**.

Table 5. Selected Bond Distances (Å) and Angles (deg) for **5**

Ag(1)−C(1)	2.117(5)	C(1)−Ag(1)−C(14)	176.8(2)
Ag(1)−C(14)	2.106(6)	N(1)−C(1)−N(2)	103.6(5)
C(1)−N(1)	1.353(7)	N(3)−C(14)−N(4)	103.5(5)
C(1)−N(2)	1.362(7)	Ag(1)−C(1)−N(1)	134.9(4)
C(14)−N(3)	1.361(8)	Ag(1)−C(1)−N(2)	121.3(4)
C(14)−N(4)	1.360(8)	Ag(1)−C(14)−N(3)	134.0(4)
		Ag(1)−C(14)−N(4)	122.4(4)

Table 6. Selected Bond Distances (Å) and Angles (deg) for **6**

Au(1)−C(1)	2.014(4)	C(1)−Au(1)−C(14)	173.78(14)
Au(1)−C(14)	2.022(4)	N(1)−C(1)−N(2)	111.6(3)
C(1)−N(1)	1.363(5)	N(5)−C(14)−N(6)	104.1(3)
C(1)−N(2)	1.367(5)	Au(1)−C(1)−N(1)	124.1(3)
C(14)−N(5)	1.345(5)	Au(1)−C(1)−N(2)	131.5(3)
C(14)−N(6)	1.364(5)	Au(1)−C(14)−N(5)	125.3(3)
		Au(1)−C(14)−N(6)	130.6(3)

the covalent radius of Au(1).[19] Neither complex shows extended intermolecular metal−metal interactions. In **5** the closest Ag···Ag interaction is 7.786 Å, while in **6** the shortest Au···Au interaction is much shorter at 4.101 Å but still considered noninteracting.

(19) Tripathi, U. M.; Bauer, A.; Schmidbaur, H. *J. Chem. Soc., Dalton Trans*. **1997**, 2865.

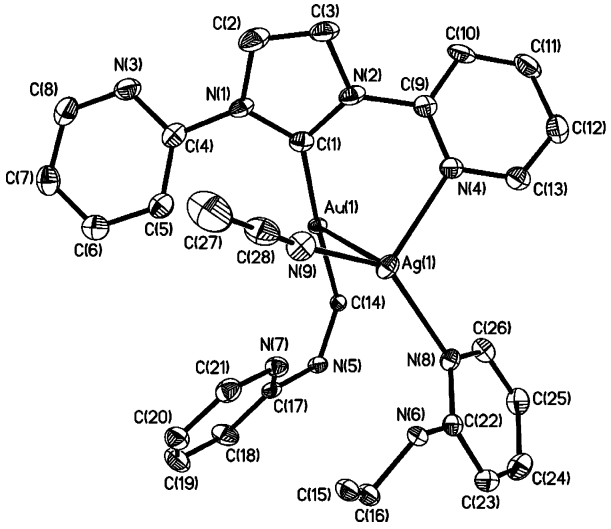

Figure 5. X-ray structural drawing depicting the cationic portion of **7** with thermal ellipsoids drawn at 50% level. Only the asymmetric unit is shown. The remainder of the polymer is symmetry generated along the 6-fold screw axis. The remaining imidazole ring is formed by symmetry combinations of N(5)−C(14)−N(6)−C(16)−C(15). Hydrogen atoms removed for clarity.

Table 7. Selected Bond Distances (Å) and Angles (deg) for **7**

Au(1)−Ag(1)	2.8359(4)	Ag(1)−Au(1)−Ag(1A)	171.80(1)
Au(1)−Ag(1A)	2.9042(4)	Au(1)−Ag(1)−Au(1B)	166.18(1)
Au(1)−C(1)	2.001(4)	C(1)−Au(1)−C(14)	176.26(16)
Au(1)−C(14)	2.014(4)	N(4)−Ag(1)−N(8)	102.02(11)
Ag(1)−N(4)	2.389(4)	N(4)−Ag(1)−N(9)	117.68(14)
Ag(1)−N(8)	2.323(4)	N(8)−Ag(1)−N(9)	138.85(13)
Ag(1)−N(9)	2.225(4)	C(1)−Au(1)−Ag(1)	79.49(12)
C(1)−N(1)	1.359(5)	C(14)−Au(1)−Ag(1)	99.87(11)
C(1)−N(2)	1.365(5)	N(4)−Ag(1)−Au(1)	75.17(9)
C(14)−N(5)	1.354(5)	N(8)−Ag(1)−Au(1)	99.24(9)
C(14)−N(6A)	1.361(5)	N(9)−Ag(1)−Au(1)	100.87(10)
		C(1)−N(2)−C(9)	124.2(3)
		N(2)−C(9)−N(4)	115.8(4)
		C(9)−N(4)−Ag(1)	126.2(3)
		Au(1)−C(1)−N(2)	125.0(3)
		C(1)−Au(1)-Ag(1)−N(4)	64.35(15)
		C(1)−N(2)-C(9)−N(4)	49.1(6)

Like **3** and **4** the addition of $AgBF_4$ to **6** dramatically changes the structure, and the extended, heterometallic coordination polymer, $\{[AuAg((py)_2im)_2(NCCH_3)]\text{-}(BF_4)_2\}_n$, **7**, is isolated as long colorless needles. As shown in Figure 5 this material crystallizes in a helical fashion, and crystal structures were serendipitously obtained on both enantiomers which crystallize in one of the chiral space groups, P6(1) or P6(5). Aside from the change in helicity these two species are identical in every respect, and only one structure warrants discussion. Selected bond distances and angles are presented in Table 7. The asymmetric unit contains a Au(I) center linearly coordinated to two carbene ligands and a Ag(I) ion coordinated to two of the pyridine rings on opposing (and alternating) carbene ligands and to an acetonitrile molecule giving the Ag(I) center a distorted trigonal coordination environment. Two tetrafluoroborate anions and an acetonitrile solvate molecule complete the crystal lattice. The helicity is introduced by the formation of the six-membered dimetallacycle containing Au(1), Ag(1), C(1), N(2), C(9), and N(4). The extended structure displays alternating Au(1)−Ag(1) separations that are very short at 2.8359(4) and 2.9042(4) Å. The gold−carbene distances are similar to those observed in **6** with Au(1)−C(1) and Au(1)−C(14) measuring 2.001(4) and 2.014(1) Å, respectively. Unlike **4** the acetonitrile molecule is strongly bound with the Ag(1)−N(9) bond distance of 2.225(4) Å, and this separation is shorter than the remaining pyridine distances of 2.389(4) and 2.323(4) Å for Ag(1)−N(4) and Ag(1)−N(8), respectively. The longer pyridine distances likely reflect the strain imposed by the rigid carbene backbone which prevents a closer approach of the pyridine groups. The sum of the angles around the Ag(1) atom at 358.55° nearly equals the 360° angle required for planarity. The Ag(1)−Au(1)−Ag(1A) and Au(1)−Ag(1)−Au(1A) angles alternate 171.804(12) and 166.176(13)° giving the extended chain a slight bend at each Ag atom as emphasized in Figure 6.

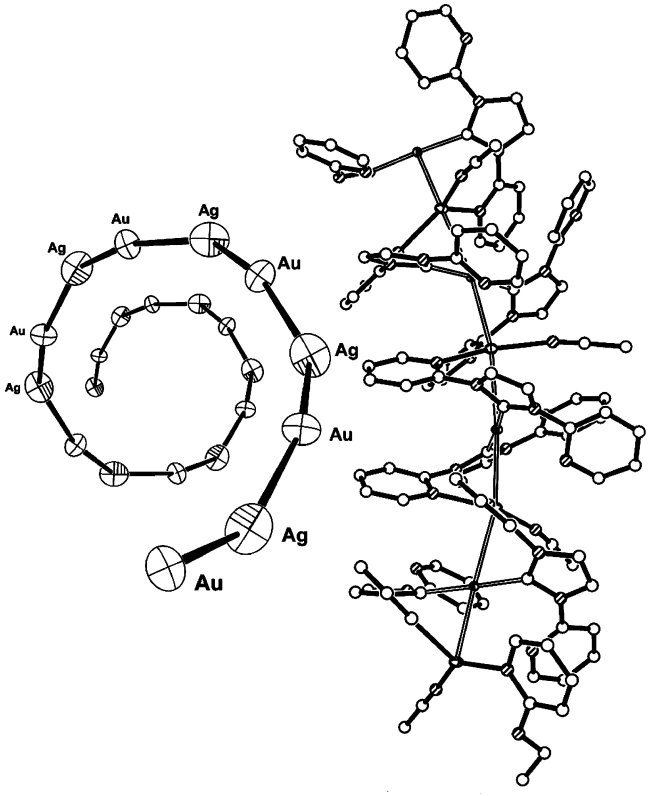

Figure 6. Crystal structure drawing showing the extended structure of one hand of **7** (right). The metal atoms can be identified by their coordination number with each Ag atom adopting a three-coordinate geometry and each gold adopting a linear, two-coordinate mode. Carbon atoms are drawn as open circles, nitrogen atoms have a diagonal line pattern, and hydrogen atoms removed for clarity. The extended, helical metal core with alternating Au−Ag separations of 2.8359(4) and 2.9042(4) Å is shown left.

The mercury containing species, **8** and **9**, have crystal structures similar to the other related homoleptic, two-coordinate d^{10} species. As shown in Figure 7 $[Hg((pyCH_2)_2\text{-}im)_2](BF_4)_2$, **8**, crystallizes in the triclinic space group P-1 with the cation and two tetrafluoroborate anions occupying the asymmetric unit. Selected bond distances and angles are presented in Table 8. The structure contains a nearly linearly coordinated Hg(II) atom with a C(1)−Hg(1)−C(16) angle of 173.5(2)° and Hg(1)−C(1) and Hg(1)−C(16) separations of 2.077(6) and 2.072(6) Å, respectively. Figure 8 shows the quinolyl-containing species, $[Hg((quinCH_2)_2im)_2](PF_6)_2$,

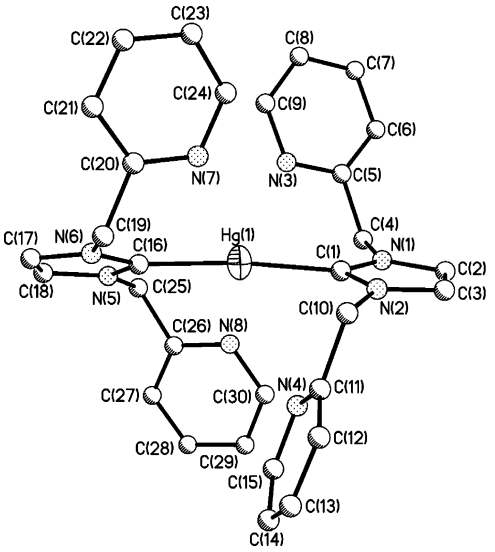

Figure 7. X-ray structural drawing depicting the cationic portion of $[Hg((pyCH_2)_2im)_2](BF_4)_2$, **8**, with carbon atoms draw as shaded circles and nitrogen atoms with dot pattern. Hydrogen atoms removed for clarity.

Table 8. Selected Bond Distances (Å) and Angles (deg) for **8**

Hg(1)−C(1)	2.077(6)	C(1)−Hg(1)−C(16)	173.5(2)
Hg(1)−C(16)	2.072(6)	N(1)−C(1)−N(2)	107.7(5)
C(1)−N(1)	1.328(8)	N(5)−C(16)−N(6)	106.9(5)
C(1)−N(2)	1.373(8)	Hg(1)−C(1)−N(1)	124.7(4)
C(16)−N(5)	1.324(8)	Hg(1)−C(1)−N(2)	127.7(5)
C(16)−N(6)	1.346(8)	Hg(1)−C(16)−N(5)	127.2(5)
		Hg(1)−C(16)−N(6)	125.9(5)

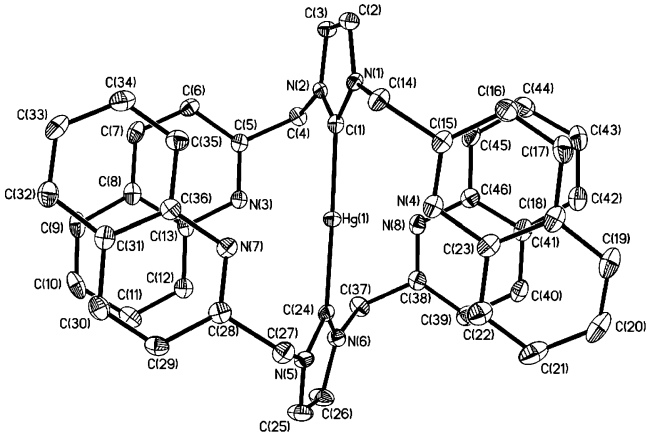

Figure 8. Thermal ellipsoid plot (50%) of the cationic portion of $[Hg((CH_2quin)_2im)_2](PF_6)_2$, **9**. Hydrogen atoms removed for clarity.

Table 9. Selected Bond Distances (Å) and Angles (deg) for **9**

Hg(1)−C(1)	2.063(3)	C(1)−Hg(1)−C(24)	173.1(1)
Hg(1)−C(24)	2.068(3)	N(1)−C(1)−N(2)	105.5(2)
C(1)−N(1)	1.338(4)	N(5)−C(24)−N(6)	106.0(2)
C(1)−N(2)	1.378(3)	Hg(1)−C(1)−N(1)	128.3(2)
C(24)−N(5)	1.347(3)	Hg(1)−C(1)−N(2)	126.2(2)
C(24)−N(6)	1.347(4)	Hg(1)−C(24)−N(5)	128.3(2)
		Hg(1)−C(24)−N(6)	125.3(2)

9, which contains a similarly coordinated Hg(II) center with Hg(1)−C(1) and Hg(1)−C(24) separations of 2.063(3) and 2.068(3) Å, respectively, and a nearly linear C(1)−Hg(1)−C(24) angle of 173.1(1)°. Selected bond distances and angles are presented in Table 9. Relative to the rest of the structure, the quinolyl groups occupy most of the space around the metal center and appear to π-stack with a quinolyl group on the opposing carbene ligand. The remaining metrical parameters are unremarkable.

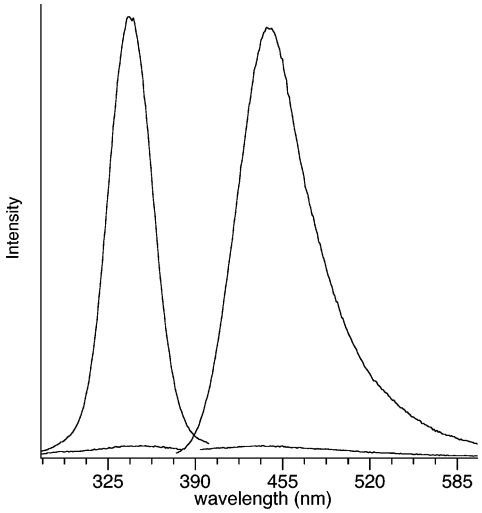

Figure 9. Solid-state emission (λ_{exi} = 346 nm) and excitation spectra of **3** (lower trace) and **4** (upper trace).

Only poor quality crystals[20] of the trimetallic $[Ag_3((quin\text{-}CH_2)_2im)_3](BF_4)_3$, **11**, were obtained, limiting the structural study. However, the triangular motif with Ag−Ag separations of 2.78 Å similar to the structure of **2** could be gleaned from the poor quality data. A crystal structure drawing and selected bond distances and angles are included as Supporting Information.

The electronic absorption spectra of complexes **3**−**11** are nearly featureless with ligand centered ($\pi-\pi^*$) absorption bands between 250 and 280 nm. The added conjugation of the quinolyl-species extends these absorption bands to ∼320 nm, and two sharp bands associated with the quinolyl group at 302 and 316 nm are resolved.

All of the compounds reported here are photoluminescent in solution as are the carbene precursors. The luminescent properties of **1** and **2** were reported elsewhere.[16] In acetonitrile, both **3** and **4** display weak emission bands at 443 nm (λ_{exi} = 346 nm), while under the same conditions the imidazolium salt $[H(pyCH_2)_2im]BF_4$ displays an unsymmetrical band at ∼400 nm that tails out to ∼550 nm. In the solid state (Figure 9), however, compound **4** is significantly more luminescent than its Ag-free precursor both of which have emission bands at 455 nm which are effectively pumped by absorptions at 340 nm. The similarity in emission maxima suggests that these processes originate from the same electronic state. Likewise, the analogous $(py)_2$im-containing complexes also show similar solution and solid-state emission properties. In acetonitrile complexes **5**−**7** and the ligand precursor all display sharp emission bands at 345 nm that originate from an electronic state centered at ∼284 nm suggesting a fluorescence process. In the solid state these emission bands shift to 520 nm for **5**, 545 nm for **6,** and 515 nm for **7** with the emission for the monometallic $[Au((py)_2im)_2]BF_4$, **6**, being the most intense. In the solid state

(20) Crystal data for $[Ag_3((quin\text{-}CH_2)_2im)_3](BF_4)_3$, **11**. Pale yellow stacked plates, $a = b = 13.515(4)$ Å, $c = 20.586(8)$ Å, $\alpha = \beta = 90°$, $\gamma = 120°$, hexagonal, P-31c, $R_1 = 0.1223$.

the emission maxima of the ligand precursor, $[H(py)_2im]BF_4$, also shifts to lower energy with a band observed at 514 nm. Compound **8** behaves similarly its Ag and Au homologues with a weak emission band observed at 445 nm ($\lambda_{exi} = 283$ nm, CH_3CN). The quinolyl species, **9**, appears slightly more emissive with its emission band centered at 390 nm ($\lambda_{exi} = 318$ nm, CH_3CN) which is nearly identical to the quinolyl ligand precursor, $[H(quinCH_2)_2im]PF_6$. The emission spectra of **10** and **11** are similar to those reported earlier for **1** and **2**. Each shows a broad band at 431 nm when excited at 349 nm (CH_3CN).

Discussion

The complexes reported here further exemplify the utility of substituted N-heterocyclic carbene ligands as ligands for d^{10} metals and as supports for generating metal−metal interactions.[21] All of the complexes reported here are air-stable and substitution inert, except for the polymeric system **7** which appears to lose Ag(I) ion in solution but reforms the polymeric chain upon precipitation. This is in contrast to the behavior of **4** which has a similar ligation about the Au and Ag centers yet does not dissociate Ag(I) ion in solution. This may be a consequence of the constrained coordination environment around the Ag center of **7** imposed by the rigid pyridyl-imidazolium linkage as opposed to **4** where the added methylene spacer significantly relieves this strain. Accordingly, the Ag-pyridine separations (2.389(4) and 2.323(4) Å) in **7** are slightly longer than those in **4** which average 2.248(13) Å. The coordinated acetonitrile molecule displays the opposite trend and is more tightly bound to the Ag center in **7** compensating for the diminished donating ability of the withdrawn pyridine rings.

The observation of short Au−Ag separations (2.8359(4) and 2.9042(4) Å) in **7** is also noteworthy particularly in contrast to **4** where the Au−Ag distances are notably longer at 3.2197(17) and 3.2819(17) Å. This discrepancy could be attributed to several factors, most simply the strain imposed by the rigid ligand backbone of **7**. However, there have been several reports recently where shorter metal−metal interactions are attributed to the incorporation of attractive dipolar interactions.[22] For example, Fackler and co-workers[22a] recently described the structures of three isomorphous $M_2(MTP)_2$ compounds where M_2 is Au_2, Ag_2, or AgAu and MTP is diphenylmethylenethiophosphinate and attributed the shortening of the Ag−Au separation (2.912 Å) relative to the homometallic separations (>3.0 Å) to a dipolar interaction. Likewise, we observed a similar metal−metal contraction in the mixed-metal metallocryptands, $[AuPdTl(P_2phen)_3](PF_6)_2$ and $[AuPtTl(P_2phen)_3](PF_6)_2$, which have shorter M−Tl separations than their homometallic counterparts.[23] Clearly, the chiral polymeric system, **7**, has a dipole moment oriented along its long crystallographic axis, whereas **4** crystallizes with a centrosymmetric orientation in the solid state (Figure 2, bottom) canceling any cooperativity between the metal centers. However, it should also be noted that short metal−metal interactions are possible in the absence of dipolar interactions as evidenced in the trimetallic $[Ag_3((quinCH_2)_2im)_3](BF_4)_3$, **11**, species which has Ag−Ag separations of only 2.78 Å. Here, each Ag−Ag bond is bridged by the carbene portion of the ligand stabilizing the triangular Ag_3 cluster.

The structures of the remaining mononuclear compounds are interesting as they demonstrate the large steric encumbrance offered by these NHC ligands. This is particularly true for the quinolyl-species, $[Hg((quinCH_2)_2im)_2](PF_6)_2$, **9**, where the twist introduced between the imidazolium rings orients the quinolyl moieties on opposite faces of the Hg center fully encapsulating the metal center. A similar, yet smaller, effect in observed in the structures of **3** and **8**.

The origin of the photoluminescence of these species is not well-understood. In the complexes with strong metal−metal interactions it is tempting to invoke a metal-centered mechanism; however, the remarkable similarity between the emission properties of the ligand precursors and their metal salts suggests that a ligand-centered emission is likely. There are relatively few reports of emission from Au− or Ag−carbene complexes. Lin and co-workers[24] reported the emission properties of a series of Au-benzimidazol-2-ylidene complexes that show dual emission bands in the solid state assigned to either an intraligand transition or a metal−metal state originating from weak intermolecular aurophilic interactions. In solution where metal−metal interactions are absent the remaining emission was assigned to an intraligand transition similar to what is observed in this work.

From a structural perspective the chiral polymer **7** is very interesting. Silver coordination polymers are well-known,[25] and helical arrays of Ag(I) centers formed from chiral ligands have also been reported.[26] However, no reports of single handed, mixed-metal species formed from achiral ligands could be found. Spontaneous resolution generating homochiral Ag-containing polymers from achiral components has been reported, but none contain short (>3 Å) Ag−Ag interactions.[27] The generation of chiral polymers through metallophilic attractions is unique, and the short Au−Ag

(21) (a) Garrison, J. C.; Simons, R. S.; Kofron, W. G.; Tessier, C. A.; Youngs, W. J. *Chem. Commun.* **2001**, 1780. (b) Melaiye, A.; Simons, R. S.; Milsted, A.; Pingitore, F.; Wesdemiotis, C.; Tessier, C. A.; Youngs, W. J. *J. Med. Chem.* **2004**, *47*, 973. (c) Barnard, P. J.; Baker, M. V.; Berners-Price, S. J.; Skelton, B. W.; White, A. H. *Dalton Trans.* **2004**, *7*, 1038.

(22) (a) Rawashdeh-Omary, M. A.; Omary, M. A.; Fackler, J. P., Jr. *Inorg. Chim. Acta* **2002**, *334*, 376. (b) Fernández, E. J.; Laguna, A.; López-de-Luzuriaga, J. M.; Monge. M.; Pyykkö, P.; Runeberg, N. *Eur. J. Inorg. Chem.* **2002**, 750. (c) Usón, R., Laguna, A.; Laguna, M.; Usón, A.; Jones, P. G.; Erdbrügger, C. F. *Organometallics* **1987**, *6*, 1778. (d) Usón, R., Laguna, A.; Laguna, M.; Usón, A.; Jones, P. G.; Sheldrick, G. M. *J. Chem. Soc., Dalton Trans.* **1984**, 285.

(23) Catalano, V. J.; Malwitz, M. A. *J. Am. Chem. Soc.* **2004**, *126*, 6560.

(24) Wang, H. M. J.; Chen, C. Y. L.; Lin, I. J. B. *Organometallics* **1999**, *18*, 1216.

(25) Khlobystov, A. N.; Blake, A. J.; Champness, N. R.; Lemenovskii, D. A.; Majouga, A. G.; Zyk, N. V.; Schröder, M. *Coord. Chem. Rev.* **2001**, *222*, 155.

(26) (a) Bowyer, P. K.; Porter, K. A.; Rae, D.; Willis, A. C.; Wild, S. B. *Chem. Commun.* **1998**, 1153. (b) Wu, B.; Zhang, W.-J.; Yu, S.-Y.; Wu, X.-T. *J. Chem. Soc., Dalton Trans.* **1997**, 1795.

(27) (a) Janiak, C.; Scharmann, T. G.; Albrecht, P.; Marlow, F.; Macdonald, R. *J. Am. Chem. Soc.* **1996**, *118*, 6307. (b) Bu, X.-H.; Chen, W.; Du, M.; Biradha, K.; Wang, W.-Z.; Zhang, R.-H. *Inorg. Chem.* **2002**, *41*, 437. (c) Abrahams, B. F. Jackson, P. A.; Robson, R. *Angew. Chem., Int. Ed. Engl.* **1998**, *37*, 2656.

separations, chiral polymeric coordination mode and photoluminescence observed in **7** open up many possibilities for optoelectronic and material applications.[28] Moreover, the presence of the uncoordinated pyridine ring and the acetonitrile molecule allow for two simple points of further modification that could fine-tune the optical and physical properties of this material. We are currently investing these systems and other multimetallic polymers based on analogous ligands.

Experimental Section

Solvents were used as received without purification or drying. The imidazolium salts, $[H(pyCH_2)_2im]BF_4$[17] and $[H(py)_2im]BF_4$[29] were prepared using an established procedure. $[H(quinCH_2)_2im]PF_6$ and $[H(quinCH_2)_2im]BF_4$ were prepared analogously to $[H(pyCH_2)_2im]BF_4$ except 2-(chloromethyl)quinoline was used in place of 2-(chloromethyl)-pyridine. The preparation of Au(tht)Cl was described elsewhere.[30] Combustion analyses were performed by Desert Analytics, Tucson, AZ. UV−vis spectra were obtained using a Hewlett-Packard 8453 diode array spectrometer (1 cm pathlength cells). Emission data were recorded using a Spex Fluoromax steady-state fluorimeter.

Preparation of $[Au((pyCH_2)_2im)_2]BF_4$, 3. A 25 mL round-bottom flask was charged with 1.00 g (1.44 mmol) of $[Ag((pyCH_2)_2im)_2]BF_4$, **2**, and 10 mL of dichloromethane. To this was added 0.461 g (1.44 mmol) of Au(tht)Cl in 5 mL of dichloromethane after which a fine white precipitate forms immediately. This mixture was stirred in the absence light for 25 min. The mixture was then filtered through Celite, and the remaining colorless solution was evaporated to dryness using a rotary evaporator. The residual white solid was dissolved in a minimum volume of CH_3CN and precipitated with Et_2O to give 0.950 g (1.21 mmol) of $[Au((pyCH_2)_2im)_2]BF_4$ as a microcrystalline product (84%). Anal. Calcd ($C_{30}H_{28}N_8AuBF_4$): C, 45.94; H, 3.60; N, 14.29. Found: C, 45.64; H, 3.55; N, 14.02. ^{1}H NMR (300 MHz, CD_3CN, 25 °C): δ = 8.44 (m, 4H), 7.66 (m, 4H), 7.30 (s, 4H), 7.23 (m, 4H), 7.16 (m, 4H), 5.41 (s, 8H). $^{13}C\{^1H\}$ NMR (75 MHz, CD_3CN, 25 °C): δ = 186.3, 156.7, 150.8, 138.4, 124.4, 123.9, 123.0, 56.9. UV (CH_3CN) λ_{max}, nm (ϵ): 237 (15900), 248 (20600), 261 (22700), 266 (sh, 19600).

Preparation of $[AuAg_2((pyCH_2)_2im)_2(NCCH_3)_2](BF_4)_3$, 4. A 50 mL round-bottom flask was charged with 0.201 g (0.256 mmol) of $[Au((pyCH_2)_2im)_2]BF_4$ and 15 mL of CH_3CN. A separate 15 mL Erlenmeyer flask was charged with 0.100 g (0.513 mmol) of $AgBF_4$ in 10 mL of CH_3CN. The $AgBF_4$ solution was then added to $[Au((pyCH_2)_2im)_2]BF_4$ slowly over 5 min. Once added, the entire mixture was stirred for 2 h. The mixture was then filtered through Celite and concentrated using a rotary evaporator. Precipitation with Et_2O affords 0.250 g (0.199 mmol) of **4** as a microcrystalline product (78%). This material can be recrystallized from CH_2Cl_2/Et_2O. Anal. Calcd ($C_{34}H_{34}N_{10}Ag_2AuB_3F_{12}\cdot CH_2Cl_2$): C, 31.35; H, 2.71; N, 10.45. Found: C, 31.84; H, 2.84; N, 9.86. ^{1}H NMR (300 MHz, CD_3CN, 25 °C): δ = 8.55 (m, 4H), 8.04 (m, 4H), 7.83 (m, 4H), 7.57 (m, 4H), 7.55 (s, 4H), 5.62 (s, 8H), 1.95 (s, 6H). $^{13}C\{^1H\}$ NMR (75 MHz, CD_3CN, 25 °C): δ = 181.1, 155.0, 152.9, 141.3, 127.1, 126.4, 124.8, 58.3. UV (CH_3CN) λ_{max}, nm (ϵ): 237 (6400), 248 (8100), 261 (9000), 265 (sh, 8000).

Preparation of $[((py)_2im)_2Ag]BF_4$, 5. A 50 mL round-bottom flask was charged with 0.207 g (0.67 mmol) of $[H(py)_2im)]BF_4$, 25 mL of CH_2Cl_2, 0.038 g of Ag_2O (0.170 mmol), and a catalytic amount of Bu_4NBF_4. The mixture was protected from light and stirred for 1 h at room temperature. NaOH (1 N, 3 mL) was then added and stirring was continued for a further 10 min. The mixture was filtered through Celite. The bright yellow filtrate was reduced to minimum volume under vacuum and precipitated with Et_2O affording 0.170 g (0.270 mmol) of **5** as a white powder (40%). Anal. Calcd ($C_{26}H_{30}N_8AgBF_4\cdot H_2O$): C, 47.52; H, 3.37; N, 17.05. Found: C, 47.20; H, 3.16; N, 16.96. ^{1}H NMR (499.8 MHz, CD_3CN, 25 °C) δ = 8.42 (m, 4H), 8.19 (s, 4H), 8.05 (m, 4H), 7.85 (m, 4H), 7.50 (m, 4H). $^{13}C\{^1H\}$ NMR (125.7 MHz, CD_3CN, 25 °C) δ = 182.7, 151.9, 149.8, 140.4, 125.2, 121.9, 116.6. UV (CH_3CN) λ_{max}, nm (ϵ): 240 (23 000), 274 (24 600), 428 (600).

Preparation of $[((py)_2im)_2Au]BF_4$, 6. A 50 mL round-bottom flask was charged with 0.104 g (0.16 mmol) of **5** and 20 mL of CH_2Cl_2. In a 25 mL Erlenmeyer flask, 0.052 g (0.16 mmol) of Au(tht)Cl was dissolved in 10 mL of CH_2Cl_2 and added to the round-bottom flask containing the solution of **5**. The mixture was protected from light and stirred for 15 min during which a precipitate forms. The solution was filtered through Celite to remove the precipitated AgCl. The clear filtrate was then reduced in volume under vacuum and precipitated using Et_2O affording 0.110 g (0.15 mmol) of **2** as a white powder (94%). Anal. Calcd ($C_{26}H_{20}N_8AuBF_4\cdot CH_2Cl_2\cdot H_2O$): C, 39.01; H, 2.91; N, 13.48. Found: C, 38.97; H, 2.98; N, 13.56. ^{1}H NMR (499.8 MHz, CD_3CN, 25 °C) δ = 8.47 (m, 4H), 7.98 (m, 4H), 7.92 (s, 4H), 7.73 (m, 4H), 7.47 (m, 4H). $^{13}C\{^1H\}$NMR (125.7 MHz, CD_3CN, 25 °C) δ = 181.2, 151.5, 150.0, 140.1, 125.7, 122.9, 119.1. (CH_3CN) $\lambda_{max,}$ nm (ϵ): 268 (23000).

Preparation of $\{[AuAg((py)_2im)_2(CH_3CN)](BF_4)_2\}_n$, 7. Method A: A 50 mL round-bottom flask was charged with 0.108 g (0.15 mmol) of **6**, 0.058 g (0.30 mmol) of $AgBF_4$, and 30 mL of CH_3CN. The colorless mixture was protected from light and stirred for 1 h. The mixture was filtered through Celite, reduced in volume under vacuum, and precipitated with Et_2O affording 0.110 g (0.11 mmol) of **7** as a off-white powder (79%).

Method B: A 50 mL round-bottom flask was charged with 0.101 g (0.139 mmol) of **6** and 0.108 g (0.55 mmol) of $AgBF_4$ in 40 mL of CH_3CN. This mixture was protected from light and brought to reflux for 9 h. The mixture was cooled, filtered through Celite, reduced to minimum volume

(28) (a) Janiak, C. *Dalton Trans.* **2003**, 2781. (b) Forward, J. M.; Fackler, J. P., Jr.; Assefa, Z. In *Optoelectronic Properties of Inorganic Compounds*; Roundhill, D. M., Fackler, J. P., Jr., Eds.; Plenum Press: 1999; p 195.
(29) Chen, J. C. C.; Lin, I. J. B. *Organometallics* **2000**, *19*, 5113.
(30) Uson, R.; Laguna, A.; Laguna, M. *Inorg. Synth.* **1989**, *26*, 85

under vacuum, and precipitated with Et_2O affording 0.120 g (0.12 mmol) of **7** as an off-white powder (86%). Crystallization from CH_3CN/Et_2O yields long colorless needles suitable for X-ray analysis. Anal. Calcd ($C_{28}H_{23}N_9AgAuB_2F_8$): C, 34.89; H, 2.40; N, 13.08. Found: C, 35.14; H, 2.78; N, 13.26. ^{1}H NMR (499.8 MHz, CD_3CN, 25 °C) δ = 8.47 (m, 4H), 7.98 (s, 4H), 7.92 (m, 4H), 7.72 (m, 4H), 7.47 (m, 4H). $^{13}C\{^1H\}$NMR (125.7 MHz, CD_3CN, 25 °C) δ = 181.0, 151.3, 150.03.8, 140.2, 125.9, 123.0, 119.2. (CH_3CN) λ_{max}, nm (ϵ): 210 (27000), 268 (19000).

Preparation of [Hg((pyCH$_2$)$_2$im)$_2$](BF$_4$)$_2$, 8. A 250 mL round-bottom flask was charged with 1.20 g (3.51 mmol) of [H(pyCH$_2$)$_2$im]BF_4 and 100 mL of CH_3CN. To this was added 0.559 g (1.75 mmol) of $Hg(OAc)_2$. The combined mixture was refluxed overnight under a nitrogen atmosphere. The mixture was cooled, and a rotary evaporator removed volatiles. The off-white residue was washed with several portions of H_2O (3 × 50 mL) and then dissolved in a minimal amount of CH_3CN. Precipitation with Et_2O gave 0.671 g (0.760 mmol) of **8** as an off-white solid (44%). X-ray quality crystals are grown by slow diffusion of benzene into a saturated acetonitrile solution of the complex. Anal. Calcd ($C_{30}H_{28}N_8HgB_2F_8\cdot H_2O$): C, 40.36; H, 3.39; N, 12.55. Found: C, 39.98; H, 3.43; N, 12.33. ^{1}H NMR (300 MHz, CD_3CN, 25 °C): δ = 8.23 (m, 4H), 7.80 (m, 4H), 7.67 (s, 4H), 7.53 (m, 4H), 7.28 (m, 4H), 5.49 (s, 8H). $^{13}C\{^1H\}$ NMR (75 MHz, CD_3CN, 25 °C): δ = 154.5, 150.9, 139.8, 125.6, 125.4, 125.2, 57.6. UV (CH_3CN) λ_{max}, nm (ϵ): 240 (15500), 247 (14000), 253 (12500), 260 (11100), 267 (7700).

Preparation of [Hg((quinCH$_2$)$_2$im)$_2$](PF$_6$)$_2$, 9. A 100 mL round-bottom flask was charged with 0.150 g (0.302 mmol) of [H(quinCH$_2$)$_2$im]PF_6 and 20 mL of CH_3CN. To this was added 0.048 g (0.151 mmol) of $Hg(OAc)_2$. This mixture was refluxed overnight under an atmosphere of nitrogen. The mixture was cooled, and rotary evaporator removed volatiles. The remaining white solid was rinsed with several portions of H_2O (3 × 30 mL) and then dissolved in a minimal amount of CH_3CN. Precipitation with Et_2O affords 0.123 g (0.103 mmol) of **9** as a white solid (68%). X-ray quality crystals are obtained by diffusion of benzene into an acetonitrile solution of the complex. Anal. Calcd ($C_{46}H_{36}N_8HgP_2F_{12}$): C, 46.38; H, 3.05; N, 9.41. Found: C, 46.69; H, 3.17; N, 9.29. ^{1}H NMR (300 MHz, CD_3CN, 25 °C): δ = 8.16 (m, 4H), 7.98 (s, 4H), 7.64 (s, 4H), 7.61 (s, 4H), 7.28 (m, 4H), 7.06 (m, 4H), 6.67 (m, 4H), 5.75 (s, 8H). $^{13}C\{^1H\}$ NMR (75 MHz, CD_3CN, 25 °C): δ = 173.8 (m), 155.5, 147.8, 140.4, 131.6, 129.3, 128.8, 128.4, 127.6, 126.1, 122.4, 57.9. UV (CH_3CN) λ_{max}, nm (ϵ): 280 (sh, 11900), 292 (12700), 304 (13100), 317 (11800).

Preparation of [(quinCH$_2$)$_2$im)$_2$Ag]BF$_4$, 10. A 100 mL round-bottom flask was charged with 0.249 g (0.568 mmol) of [H(quinCH$_2$)$_2$im]BF_4, 20 mL of CH_2Cl_2, and a catalytic amount of $[Bu_4N]BF_4$. To this was added a mixture of 20 mL of 1 M NaOH and 0.033 g (0.142 mmol) of Ag_2O. The flask was removed from light and the mixture was stirred at room temperature for 4 h. The organic layer was separated and the aqueous layer was extracted with CH_2Cl_2 (3 × 20 mL). The organic layers were combined, dried with $MgSO_4$, filtered through Celite, reduced in volume, and precipitated with Et_2O yielding 0.203 g (0.227 mmol) of **10** as a white powder (80%). ^{1}H NMR (300 MHz, CD_3CN, 25 °C): δ = 7.98 (d, 4H), 7.74−7.67 (m, 8H), 7.57 (m, 4H), 7.48 (m, 4H), 7.32 (s, 4H), 7.10 (d, 4H), 5.43 (s, 8H). $^{13}C\{^1H\}$ NMR (75 MHz, CD_3CN, 25 °C): δ = 155.2, 146.8, 136.8, 129.4, 128.3, 127.2, 126.9, 126.4, 122.2, 118.9, 56.7.

Preparation of [Ag$_3$((quinCH$_2$)$_2$im)$_3$](PF$_6$)$_3$, 11. Method A: A 100 mL round-bottom flask was charged with 0.204 g (0.411 mmol) of [H(quinCH$_2$)$_2$im]PF_6 and 0.800 g (3.45 mmol) of Ag_2O in 40 mL of CH_3CN. This mixture was protected from light and heated to reflux for 8 h. The mixture was cooled, filtered through Celite, reduced in volume, and precipitated with Et_2O affording 0.189 g (0.116 mmol) of **11** as an off-white powder (49%). Method B: A 25 mL round-bottom flask was charged with 0.04 g (0.042 mmol) of **10**, 0.021 g (0.084 mmol) of $AgPF_6$, and 20 mL of CH_3CN. The mixture was removed from light and brought to reflux for 2 h. The mixture was cooled, filtered through Celite, reduced in volume, and precipitated with Et_2O affording 0.073 g (0.040 mmol) of **11** as an off-white powder (96%). Anal. Calcd ($C_{69}H_{54}N_{12}Ag_3P_3F_{18}$): C, 45.79; H, 3.01; N, 9.29. Found: C, 46.20; H, 3.09; N, 9.22. ^{1}H NMR (300 MHz, CD_3CN, 25 °C): δ = 8.51 (d, 6H), 8.00 (d, 6H), 7.51−7.44 (m, 18H), 7.07 (m, 6H), 6.62 (m, 6H), 4.76 (AB quartet, 12H). $^{13}C\{^1H\}$ NMR (126 MHz, CD_3CN, 25 °C): δ = 156.0, 147.2, 141.1, 132.4, 129.8, 129.6, 128.6, 127.8, 127.5, 123.1, 56.2. UV (CH_3CN) λ_{max}, nm (ϵ): 280 (18800), 292 (19700), 304 (20300), 317 (18100).

X-ray Data Collection. Suitable crystals of **3**, **4**, and **8** were coated with epoxy cement, mounted on a glass fiber, and placed on a Siemens P4 diffractometer. The data were corrected for Lorentz and polarization effects. Calculations were performed using Siemens SHELXTL PLUS, version 5.03, system of programs refining on F^2. The structures were solved by direct methods. An absorption correction was applied using an empirical model derived from psi scans. Hydrogen atom positions were calculated using a riding model with a C−H distance fixed at 0.96 Å and a thermal parameter 1.2 times the host carbon atom.

The remaining structures (**5**, **6**, **7**, and **9**) were collected at low temperature using a Bruker SMART Apex CCD diffractometer with Mo Kα radiation and a detector-to-crystal distance of 4.94 cm. Data were collected in a full sphere using four set of frames with 0.3° scans in ω with an exposure time of 10s per frame. The 2θ range extended from 3.0 to 64°. Data were corrected for Lorentz and polarization effects using the SAINT program and corrected for absorption using SADABS. Unit cells were indexed using reflections harvested from the data collection. The structures were solved by direct methods and refined using the SHELXTL 5.12 software package.[31]

Acknowledgment. This work and the X-ray diffractometer purchase were supported by the National Science Foundation (CHE-0091180 and CHE-0226402). We are

(31) XRD Single-Crystal Software; Bruker Analytical X-ray Systems: Madison, WI, 1999.

grateful to Prof. Marilyn M. Olmstead for her assistance with the X-ray crystallography.

Supporting Information Available: Structural drawing of bond distances and angles for **11** and crystallographic data in CIF format for **3**−**9.** This material is available free of charge via the Internet at http://pubs.acs.org.

IC049604K